Influence of ozone supply mode and aeration on photocatalytic ozonation of organic pollutants in wastewater using TiO$_2$ and ZnO nanoparticles

Reyhaneh Nabizadeh [a,b], Rezvaneh Amrollahi [a], Bijan Ghafary [a], Shahab Norouzian Alam [a,b,*]

[a] *Physics Department, Iran University of Science and Technology, Tehran, Iran*
[b] *Optoelectronics Research Center, Iran University of Science and Technology, Tehran, Iran*

ARTICLE INFO

ABSTRACT

Photocatalytic ozonation, which combines the effects of lighting and ozonation, has been shown to enhance the decolorization and degradation of organic pollutants in wastewater. Dye solutions with concentrations of 10 ppm for both methylene blue and methyl orange dyes were used. The influence of ozoneation on the performance of photocatalytic activity of TiO$_2$ and ZnO nanoparticles for the removal of organic dyes from aqueous solutions was investigated. To evaluate their efficacy for the removal of methylene blue and methyl orange dyes from aqueous solutions, the photocatalysts were exposed to UV light for 90 min, with ozone supplied either intermittently or continuously by an SDBD cold plasma reactor. The photocatalysts utilized in this study were characterized using SEM and XRD techniques. The degree of color degradation was determined using UV–Vis spectroscopy. The results demonstrate that TiO$_2$ and ZnO nanoparticles exhibit different degrees of photocatalytic activity for the two dyes. The addition of ozone was found to enhance both the color degradation and mineralization rates of the pollutants, with intermittent ozonation proving more effective than continuous ozonation. The most significant color degradation results were obtained using TiO$_2$ nanoparticles with intermittent ozonation for methylene blue dye (97 %) and ZnO nanoparticles with intermittent ozonation for methyl orange dye (40 %). Overall, this study provides evidence that photocatalytic ozonation represents a promising technique for water treatment.

1. Introduction

Water pollution is a global issue that affects human health and the environment. One of the leading causes of water pollution is the presence of organic compounds from various industries, such as pharmaceuticals, cosmetics, and dyes. These compounds are often toxic, persistent, and resistant to conventional wastewater treatment methods. Therefore, there is a need to develop new techniques that can effectively and sustainably remove these compounds from wastewater [1–3].

Various methods are used for wastewater treatment, including Fenton's chemical oxidation, electrochemical decomposition, cation exchange membranes, filtration, nanofiltration [4], coagulation, reverse osmosis, chemical separation of pollutants, surface adsorption

---

* Corresponding author. Physics Department, Iran University of Science and Technology, Tehran, Iran.
E-mail address: norouzian@iust.ac.ir (S. Norouzian Alam).

Table 1

Synergy of ozone and photocatalyst for wastewater treatment.

pollutant	Time(min)	Photocatalyst/Catalyst	Ozone rate	Removal (%)	Reference
Basic Yellow 87	240	$ZrO_2/Al_2O_3/ZnO/Cu$	0.5 (l/min)	99	[29]
Total organic carbon(TOC)				30	
Chemical Oxygen Demand				59	
Terfetalic Acid	3.66	$MnFe_2O_4$/Willemite	2.17 (mg/h)	98.3	[30]
salicylic acid	60	ZnO/TiO_2	30 (ml/min)	64.4	[26]
Paraben	20	ZnO	1.1 (g/h)	100	[31]
Textile dyeing wastewater	480	Cu/ZnO	0.44 (g/h)	95.4	[32]
TOC				80	
Chemical Oxygen Demand				95	
Phenol	60	ZnO	50 (ml/min)	86	[33]
TOC				10	
Phenol	60	Ag/ZnO	50 (ml/min)	100	[33]
TOC				52	
Textile dyeing wastewater	30	ZnO/Cu	0.48 (g/h)	98	[34]
MB(without aeration)	45	TiO_2	200 (bubble/min)	96	This work
MB(with aeration)	20	TiO_2	200 (bubble/min)	79	This work
	45			98	

on activated carbon, biological purification, and photocatalyst [5]. However, these methods aren't always efficient and have disadvantages such as high cost and high energy consumption. They also don't eliminate pollutants and cause their transfer from one phase to another, which requires further purification; complementary techniques must be used to achieve extraordinary results. One of the new methods is advanced oxidation processes (AOPs), which use highly reactive species such as hydroxyl radicals (OH), superoxide (O_2^-), and ozonide (O_3^-), and electron-hole pairs to break down the organic compounds into harmless substances or carbon dioxide and water [6–8]. Since combined techniques generally aim to treat all possible contaminants, AOPs are the best choice due to their efficient and non-selective performance. Almost all organic pollutants can be easily degraded using advanced oxidation processes, even when they are difficult to degrade by conventional methods. Heterogeneous photocatalysts, radiation-induced degradation, ozonation, sonolysis, and Fenton process are AOP techniques that are often used for pollutant oxidation [9,10].

Two of the most widely used AOPs are ozonation and photocatalysis [11–13]. Ozonation uses ozone molecules to oxidize organic compounds directly or indirectly. Photocatalysis uses a semiconductor material (such as ZnO or TiO_2) that produces electron-hole pairs when exposed to light [14–20]. These electron-hole pairs can then react with water or oxygen to generate OH radicals or other species that can oxidize the organic compounds [21,22].

Both ozonation and photocatalysis have advantages and disadvantages. Ozonation has a high oxidation potential and can degrade many organic compounds [23–25]. Still, it also has a high production cost, low solubility and stability in water, a selective reaction at acidic pH, and incomplete mineralization of some compounds. Photocatalysis has a low production cost, high stability in water, a non-selective reaction at any pH, and a complete mineralization of some compounds. Still, it also has a slow reaction rate, a charge recombination problem, a poor mass transfer of fixed catalysts, and a limited light absorption range. To solve these problems, ozonation and photocatalysis can be combined to form a synergistic process called photocatalytic ozonation. This process can increase oxidation efficiency and reduce ozone consumption by improving the generation of OH radicals [26–28].

Many studies on wastewater treatment are using advanced oxidation methods, especially photocatalytic and ozonation methods. In the following, we study some of the works done on the synergistic effect of these two technologies in destroying pollutants. Table 1 shows the results of recent research on the synergy of ozonation and photocatalyst. From the analysis of these data and the comparison of the results of this research, it can be seen that adding air to the photocatalytic setup during ozonation increases the rate of pollutant degradation.

So that there isn't a need to modify TiO_2 nanoparticles and preparation before the process, and only by adding air to the solution, wastewater treatment is improved.

Recently, studies have been conducted on the effectiveness of ozonation on wastewater treatment, and the effectiveness of this method was investigated along with other advanced oxidation processes. The results showed that the combination of ozone and photocatalyst gave better results than the combined O_3/UV, O_3/H_2O_2, O_3/catalyst, and ozonation and photocatalyst processes alone [26,35].

98 % removal of terephthalic acid was observed by $UV/MnFe_2O_4$/Willemite in 3.66 min [30,36]. Also, salicylic acid was degraded by 64.4 % by 7 at% Zn–TiO_2 photocatalyst after 60 min [31]. The dyeing effluent was degraded by Cu–ZnO photocatalyst to the extent of 95.4 % after 480 min [34,32] and we see 100 % removal of phenol by Ag/ZnO after 60 min [33].

It should be noted that the results of Table 1 are for different intensities of radiation and different rates of ozone and different photocatalysts, also the concentrations of the solvents and the chemical formula of the solvents are different, but studies show that the synergy of the two advanced oxidation methods of ozonation and photocatalyst improves the photocatalytic activity in wastewater treatment.

However, to improve the efficiency of wastewater treatment and according to different ozonation methods, in this work, we also investigated two modes of continuous ozonation during the reaction time and intermittent ozonation at certain times. In this work, we propose to add aeration to the ozonation and photocatalyst processes to increase the speed of the pollutant decomposition reaction and

show that adding air to this process can be a suitable alternative for various methods to improve the efficiency of the photocatalyst (including nanoparticle doping, nano synthesis composite, pre-reaction treatment, etc.). The results showed that aeration can give more dye degradation efficiency in less time. Improvement of photocatalytic ozonation for dye degradation by adding air hasn't been investigated so far.

One of the critical factors in photocatalytic activity is the choice of the appropriate photocatalyst, so we will continue to examine the photocatalysts used in wastewater treatment. Several photocatalytic materials are used in wastewater treatment, including metal oxides, perovskite oxides, vanadates, tungstates, transition metal sulfides, graphite carbon nitride, transition metals, and nano-composites. Among these, metal nano oxides are the most common semiconducting photocatalysts due to their significant specific surface area, broad solar spectrum absorption, chemical stability, non-toxicity, abundance, and cheapness. Recent research has introduced various inorganic semiconductor nanomaterials, including ZnO, ZnS, Wo_2, CdS, SiO_2, TiO_2, Fe_2O_3, Al_2O_3, and ZrO_2 as efficient photocatalysts [37]. The most commonly used photocatalysts are ZnO and TiO_2, which are non-toxic, cheap, and photochemically stable, and are commercially available in different crystalline forms and particle properties. In the following, we will examine some features of ZnO and TiO_2.

TiO_2 is a semiconductor that is very common due to its chemical stability, non-toxicity, cheapness, optical properties, abundance, and many applications. It is known with three different crystal phases: anatase, rutile, and brookite. It exhibits good photocatalytic properties under ultraviolet light irradiation and has high photocatalytic activity in the anatase phase. TiO_2 is a semiconductor with a large band gap. Its anatase structure has an indirect band gap equal to 2.3 eV with an absorption edge at 387.5 nm, which, according to this absorption wavelength, is clear that this material has optical absorption only in the ultraviolet region (100–400 nm). Rutile has a straight and smaller band gap than anatase and is equal to 3.05 eV. The absorption edge of TiO_2 in the rutile phase is 406.5 nm and has absorption in the visible region (400–700 nm). Brookite, with a band gap of 2.96 eV, can absorb wavelengths in the visible area. Anatase-type TiO_2 has a high photocatalytic activity for decomposing various environmental pollutants in gas and liquid phases [18].

The critical reasons for the widespread use of TiO_2 in photocatalytic processes are 1. High light absorption power, 2. Relatively low synthesis price, 3. Structural features include an indirect band gap (in the anatase phase), 4. Physical and chemical stability under reaction conditions (stability against optical corrosion), 5. Non-toxicity, 6. The high oxidation power of the holes is produced with the help of photons [16,38,39].

ZnO has three primary crystal forms including hexagonal wurtzite, cubic zinc blende, and cubic rocksalt. Wurtzite structure is more stable and familiar in environmental conditions. ZnO has a wide band gap of about 3.3 eV. As a photocatalyst, ZnO has essential advantages such as low price and high photocatalytic activity. The most significant advantage of ZnO is that it absorbs a more significant part of the UV spectrum than TiO_2. The optical stability of ZnO is lower compared to TiO_2, also due to the direct band gap of this semiconductor, it is expected that the rate of electron-hole recombination in it is higher than that of TiO_2 and this is the main reason for the broader use of TiO_2 than ZnO in environmental processes and wastewater purification [19,20].

Some semiconductor materials create a synergistic effect between photocatalyst and ozonation to greatly improve the oxidation efficiency of organic pollutants. TiO_2 is a widely used photocatalyst for photocatalytic ozonation of organic materials due to its unique properties such as easy fabrication, low cost, non-toxicity, high chemical stability, high stability, and good photoreactivity, strong oxidation power [40]. Therefore, in this article, we use TiO_2 and ZnO as photocatalysts and industrial dyes as the target pollutants, which we will learn about later.

One of the main factors of wastewater pollution is dyes used in various textile, leather, plastic, paper, concrete, pharmaceutical and cosmetic, food, and medical industries. These dyes usually contain toxic compounds and harm the health of humans, aquatic animals, and the environment. Methylene blue (MB) is a cationic dye typically used to dye silk, wool, and cotton. Methyl orange (MO) is an anionic dye from the azo dye category, which is widely used in the dyeing industry and is very toxic, carcinogenic, and harmful to the environment and organisms. Therefore, it is necessary to remove these dyes from the wastewater that enters nature. For this reason, in this work, the degradation of MO and MB dyes as industrial wastewater pollutants has been investigated [41–43].

This study aims to evaluate the performance of photocatalytic ozonation as a means of wastewater treatment, focusing on the degradation efficiency of two model organic pollutants, MB and MO, derived from different industrial sources. The study employs ZnO and TiO_2 nanoparticles as photocatalysts and utilizes UV radiation from a mercury lamp to activate photocatalysis. Additionally, ozone is generated from the air using a plasma reactor based on cold plasma technology. The degradation efficiency of the dyes is compared under different experimental conditions, including ozonation mode (continuous or intermittent), aeration, and photocatalyst type. Finally, a proposed mechanism of photocatalytic ozonation is presented based on study results. This paper is structured as follows: Section 2 provides a comprehensive description of the materials and methods employed in the study; Section 3 presents the results and discussion in detail; Section 4 summarizes the main conclusions drawn from the study and provides recommendations for future research.

2. Experimental

2.1. Materials

All the Chemicals used in this work were analytical grade reagents and used without further purification. Deionized water was used to prepare all solutions. The cationic dye methylene blue (MB) (CI No. 52015, CAS 61-73-4) with the chemical formula $C_{16}H_{18}ClN_3S$ and molecular weight of 319.85 g/mol and the anionic dye methyl orange (MO) (CI No. 13025, CAS 547-58-0) with the chemical formula $C_{14}H_{14}N_3NaO_3S$ and molecular weight of 327.34 g/mol, were used as model pollutants in this study. Titanium dioxide (TiO_2) nanoparticles(CAS 1317-70-7) with an anatase crystal phase and a particle size of 30–50 nm and molecular weight of 79.87 g/mol and
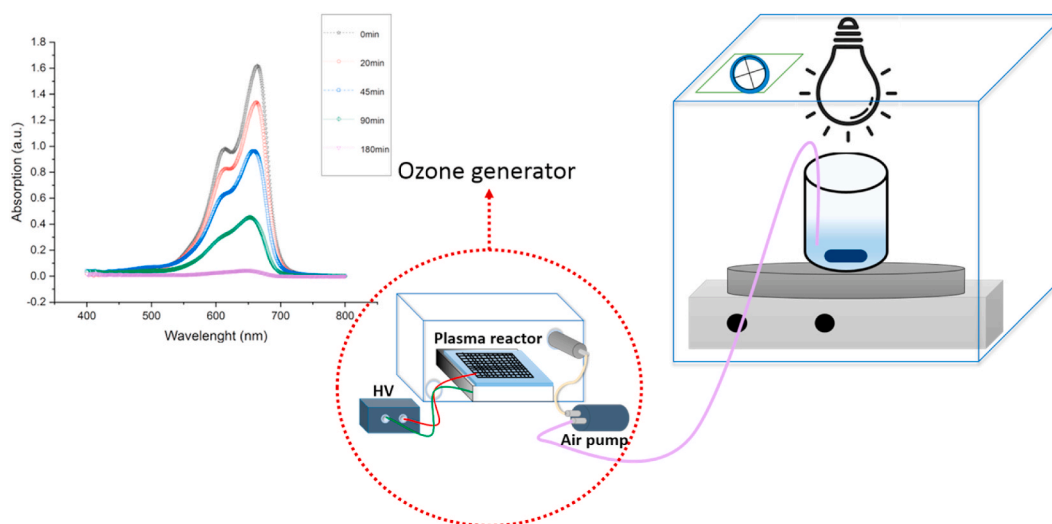
Fig. 1. Schematic diagram of photocatalytic and ozonation reactor for dye degradation.

zinc oxide (ZnO) nanoparticles(CAS 1314-13-2) with a particle size of less than 70 nm and molecular weight of 81.39 g/mol, were used as photocatalysts [44,45].

2.2. Preparation

To evaluate the photocatalytic activity, 50 ml of dye solutions with a concentration of 10 ppm were mixed with 0.05 g of the photocatalyst. The mixture was in the dark on a shaker for 25 min to reach the adsorption-desorption equilibrium. To prevent light absorption, the container holding the solution and the photocatalyst was wholly wrapped with aluminum foil. Then, each sample was exposed to a mercury lamp for 90 min. The solutions were sampled at 0, 20, 45, and 90 min after light exposure. All samples were stored in the dark and then analyzed by UV/Vis spectroscopy to measure their absorption spectra.

2.3. Characterization

X-ray diffraction (XRD) pattern was used to confirm the crystal structure of the samples in the range of $2\theta = 5–80°$. XRD analysis was performed on a D Jeoljdx-8030 X-ray powder diffractometer with Cu Kα ($\lambda = 0.15406$ nm) radiation (40 kV, 30 mA). Scanning electron microscopy (SEM) was employed to investigate the microstructure, morphology, and particle distribution of the samples. Ultraviolet–visible spectroscopy was performed on all the samples and the changes in dye concentration and degradation efficiency were calculated from the UV–Vis spectra of the samples. Spectrophotometrically using a double-beam UV–Vis spectrometer (Shi-madzuUV-1700) at room temperature in 200–800 nm [46].

2.4. Ozone generator

Dielectric barrier discharge (DBD) is one of the common sources of cold plasma ozone generators [47]. In DBD plasma, two electrodes separated by a dielectric material are subjected to a very high voltage. This creates a high potential difference that accelerates the electrons from the cathode to the anode. The electrons collide with gas molecules and cause them to be excited and ionized. This leads to the optical breakdown of the gas, which becomes a quasi-neutral medium with charged particles, ions, and neutral atoms. When the excited atoms return to a stable state, they emit ultraviolet rays. The collision of energetic electrons with molecules also generates free radicals, reactive oxygen species, nitrogen oxides, etc [48,49]. These free radicals and active molecules have strong oxidizing properties. Ozone is one of the free molecules formed due to the interaction of air or pure oxygen with plasma. Dielectric barrier discharge plasma is used in surface and volume structures [47,49–52].

Fig. 1 illustrates the schematic of photocatalytic ozonation in this research, where a plasma reactor was used as a source of ozone generators. We used surface dielectric barrier discharge (SDBD) plasma as the source of the ozone generator in this study. To produce SDBD plasma, we used a hollow cube with two open ends measuring $2 \times 12 \times 9$ cm as a high-voltage electrode and cooling system, ordinary glass with a thickness of 2 mm as a dielectric material, and a galvanized mesh as a grounded electrode. The aluminum cube was designed such that the airflow could pass through it and keep the glass temperature low. We also developed a cubic box made of plexiglass with a thickness of 2.8 mm and dimensions of $20 \times 20 \times 10$ cm as the ozone generator chamber. We used an air pump to deliver the ozone flow into the sample solutions. The air pump was regulated by the power supply to achieve the optimal mode and the mildest airflow conditions.
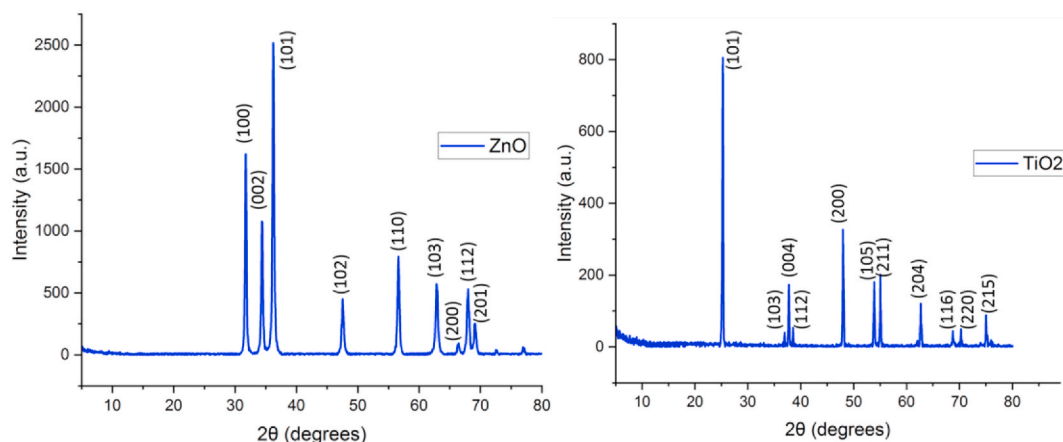
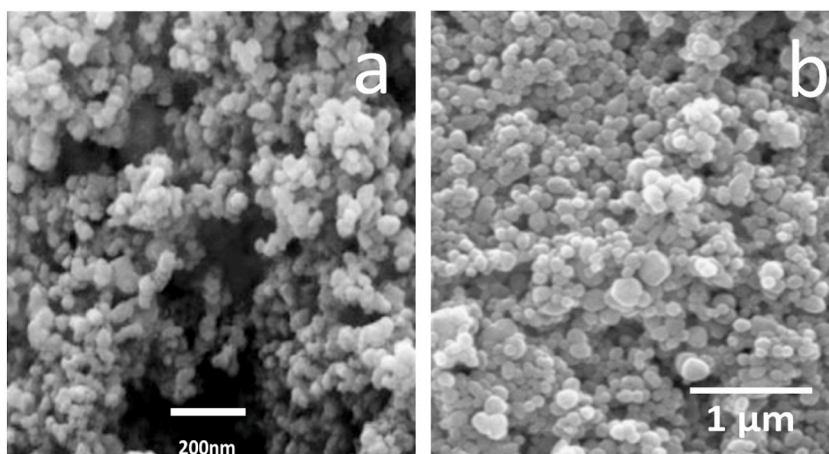**Fig. 2.** XRD diagram of (a)TiO$_2$ nanoparticles, (b)ZnO nanoparticles.

Fig. 3. (a) SEM images TiO$_2$ nanoparticles, (b) SEM images ZnO nanoparticles.

2.5. Photocatalysis and photocatalytic ozonation experiments

2.5.1. Photocatalysis

The photocatalytic activity of ZnO nanoparticles and TiO$_2$ nanoparticles to degrade MB and MO dyes, which are model pollutants, was evaluated under mercury lamp irradiation with a wavelength range of 400–800 nm. The electrons are excited with higher energy levels as the pressure inside the lamp increases, and the lamp's light gradually becomes more visible. All the samples were placed in the dark on a shaker before irradiation to reach the adsorption equilibrium. The samples were irradiated for 90 min while placed on a magnetic stirrer to maintain the homogeneity of the solution.

2.5.2. Photocatalytic ozonation

The samples were ozonated in three ways: continuously, intermittently, and with air. The intermittently ozonated samples were treated for 10 min at a rate of 200 bubble/min before and after shaking. The continuously ozonated samples were also exposed to the same ozone flow rate during the experiment. Some samples were aerated constantly with a flow rate of 200 bubble/min and increased to 400 bubble/min for 1 min every 5 min to examine the effect of oxygen amount in the sample on photocatalytic ozonation. The suspensions were analyzed before and after irradiation.

3. Results and discussion

3.1. Structure

The crystal structure of ZnO and TiO$_2$ nanoparticles was determined by obtaining the X-ray diffraction pattern as a peak intensity diagram in terms of angle 2θ with a range of 5–80° under X-ray radiation using an X-ray diffraction spectrometer.

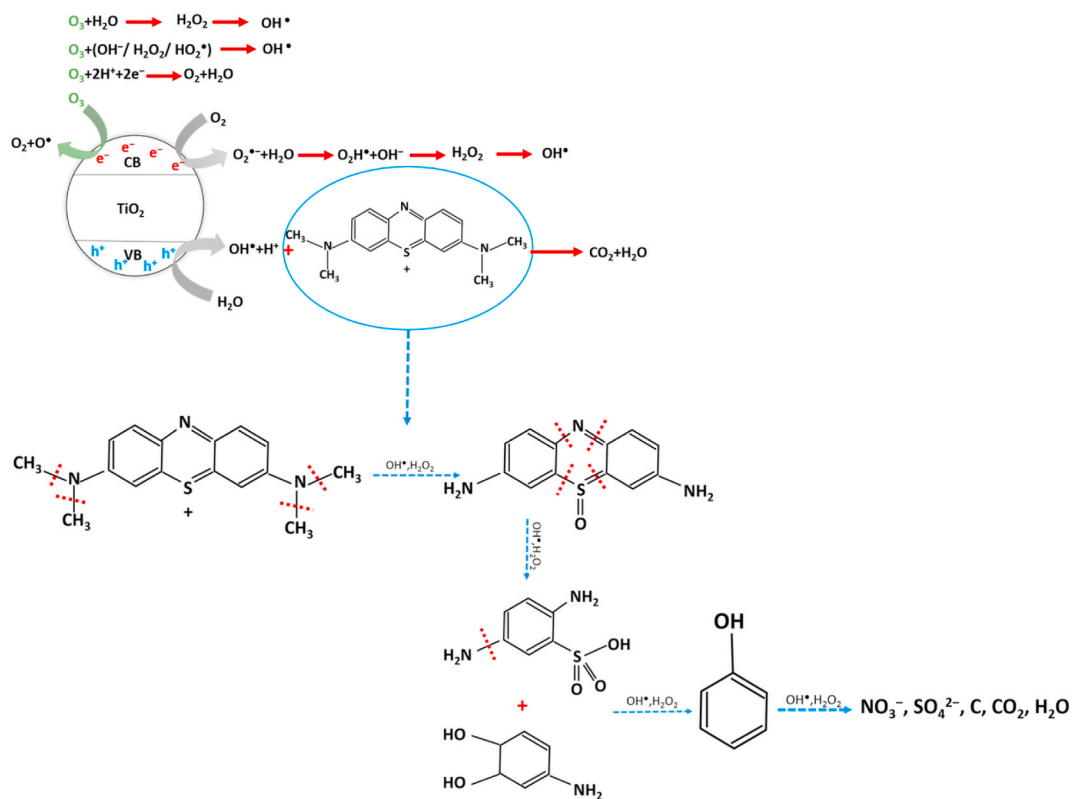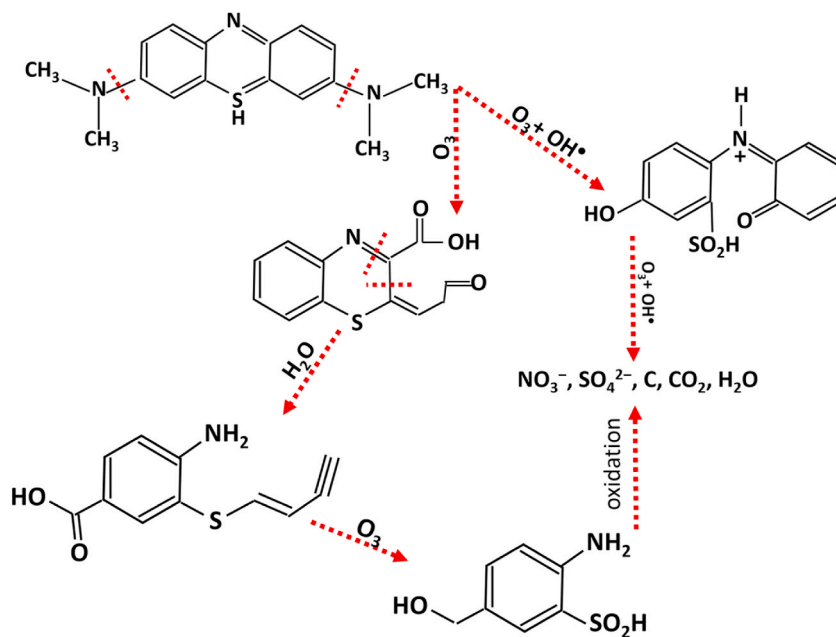**Fig. 4.** Proposed MB degradation pathway during the photocatalytic process.

Fig. 5. The path of degradation mechanism of MB dye in the presence of ozone.

Fig. 2(a) shows the XRD spectrum of TiO_2 nanoparticles, whose peaks at 2θ are 25.28, 37.76, 36.99, 38.56, 48, 53.88, 55.04, 62.68, 68.76, 70.28, and 75.04, which are respectively attributed to the planes (101), (103), (004), (112), (200), (105), (211), (204), (116), (220) and (215).

Table 2
Degradation percentage of MB dye under UV radiation.

Sample	20 min	45 min	90 min
ZnO, MB	18 %	42 %	75 %
ZnO, MB, O_3 (Continuous)	16 %	39 %	75 %
ZnO, MB, O_3 (Intermittent)	16 %	42 %	80 %
TiO_2, MB	39 %	76 %	96 %
TiO_2, MB, O_3 (Continuous)	58 %	95 %	97 %
TiO_2, MB, O_3 (Intermittent)	68 %	96 %	97 %
TiO_2, MB, Air	56 %	86 %	93 %
TiO_2, MB, Air, O_3	79 %	95 %	98 %
MB	4 %	7 %	14 %
MB, O_3	35 %	8 %	16 %

Table 3
Degradation percentage of MO dye under UV radiation.

Sample	20 min	45 min	90 min
ZnO, MO	10 %	20 %	31 %
ZnO, MO, O_3 (Continuous)	1 %	16 %	26 %
ZnO, MO, O_3 (Intermittent)	14 %	20 %	40 %
TiO_2, MO	11 %	15 %	18 %
TiO_2, MO, O_3 (Continuous)	3 %	10 %	9 %
TiO_2, MO, O_3 (Intermittent)	9 %	19 %	25 %

The strong diffraction peaks at 25° and 48° indicate TiO_2 in the anatase phase. No false diffraction peaks were found in the sample, and the two peaks at 25.28° and 48° confirm its anatase structure [53]. Fig. 2(b) shows the XRD spectrum of ZnO nanoparticles whose peaks at 2θ are equal to 31.76, 34.36, 36.24, 47.52, 56.6, 62.84, 66.44, 67.96, 69.12, and 76.92, which are respectively attributed to the planes (100), (002), (101), (102), (110), (103), (200), (112) and (201) [54].

The microstructure and distribution of nanoparticles can be seen with the help of a scanning electron microscope. Fig. 3 shows the morphology of ZnO and TiO_2 nanoparticles. As it is evident in both images, the size of all nanoparticles is almost the same, and the nanoparticles are uniform in terms of particle size. Also, in terms of shape, all nanoparticles are almost identical and spherical. As seen in the figure, the size of TiO_2 particles is around 30–50 nm, and the size of ZnO particles is less than 70 nm.

3.2. Ozonation activity

3.2.1. Effect of ozone on photocatalytic activity

The dye degradation of the samples that were ozonated was higher than that of the samples that only had photocatalysts in general [55]. Therefore, according to the chemical reactions of MB dye degradation due to photocatalytic activity and in the reaction with ozone shown in Figs. 4 and 5, it is expected that the percentage and speed of dye degradation will increase with the synergy of these methods.

Fig. 4 shows the photocatalytic process for the decomposition of MB dye. Therefore, MB undergoes chain reactions of oxidation and reduction and response with highly reactive OH^+ and H_2O_2 molecules to become safe compounds of NO_3^-, SO_4^{2-}, C, CO_2, and H_2O.

As shown in Fig. 5, the decomposition of MB in the presence of ozone is also carried out during a chemical reaction with ozone, water, hydroxyl radical, and oxidation reaction, and after several stages of chemical reaction, harmless compounds remain.

The photocatalytic activity under different ozonation conditions was investigated as continuous and intermittent ozonation. The samples that were intermittently ozonated showed better dye degradation efficiency in the first 45 min of exposure. The samples that were continuously ozonated showed higher dye degradation efficiency after 90 min. Tables 2 and 3 show the percentage of dye degradation after 20, 45, and 90 min of UV radiation, with varying conditions of photocatalyst type, ozone presence, and ozonation model.

According to Tables 2 and in general, the degradation of MB by TiO_2 photocatalyst is better than ZnO. The degradation of MB after 20 min by TiO_2 photocatalyst and the absence of ozone is 39 %. In the case of continuous ozonation and intermittent ozonation, it increased to 58 % and 68 %, respectively; however, after aeration and ozonation, the dye degradation increased to 79 %.

According to Tables 3 and in general, the ZnO nano photocatalyst showed better dye degradation for MO, and ozonation improved the dye degradation by ZnO, but it had no particular effect on TiO_2 activity. Most dye degradation was done by ZnO and intermittent ozonation, and after 20 and 90 min, 14 % and 40 % dye degradation were achieved, respectively.

Fig. 7 shows the graph of MB degradation by TiO_2 under different ozonation conditions. The addition of ozone as a strong oxidant improved the photocatalytic degradation performance of MB; considering the relatively better degradation of the dye by TiO_2 for this compound, an experiment was designed to investigate the effect of aeration in the solution in addition to ozonation.

Firstly, the photocatalytic activity of dye degradation only with aeration and without ozonation was investigated. Then, the aerated sample continuously was ozonated for 1 min at 5-min intervals. The result of MB degradation in all different laboratory conditions is
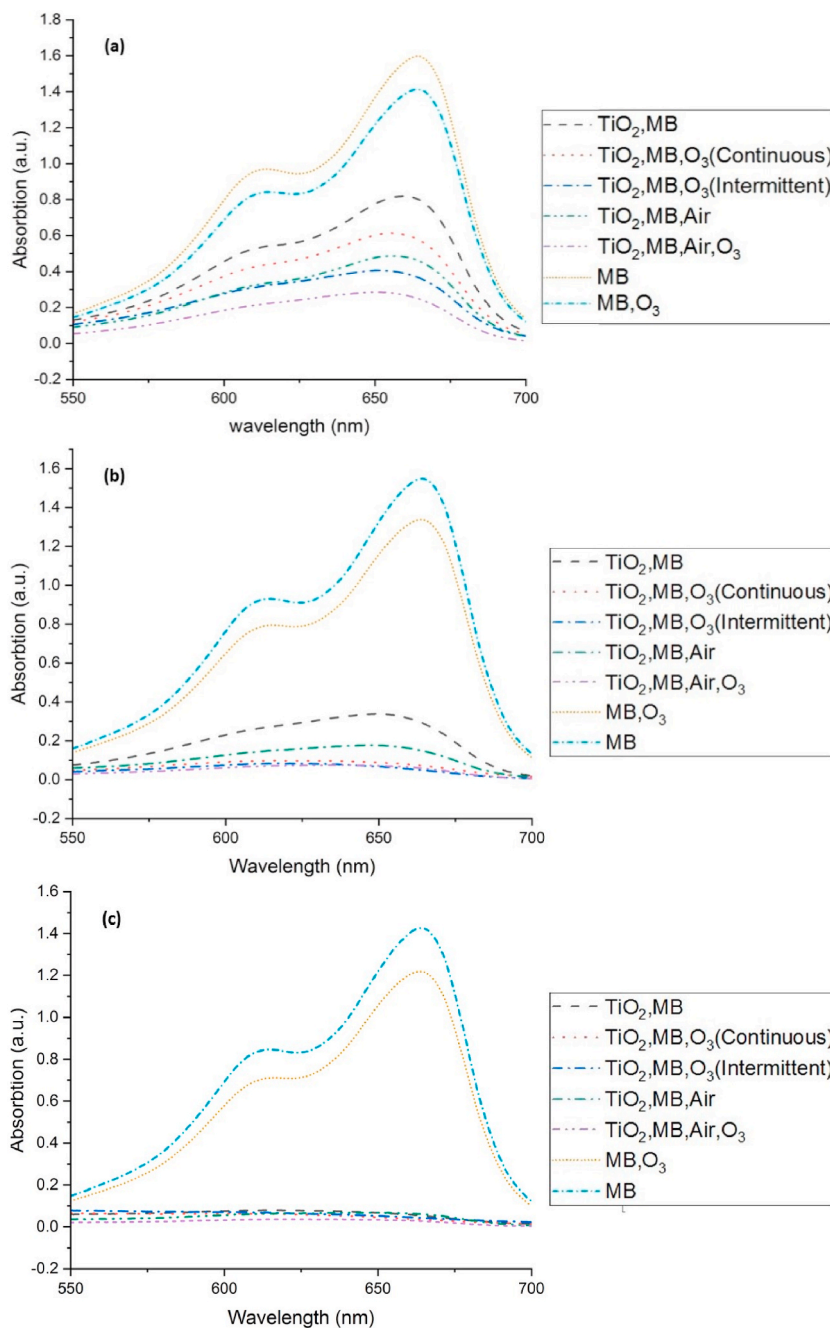
Fig. 6. UV–Vis diagram of (MB, TiO$_2$) solutions after, (a) 20 min, (b) 45min, (c) 90 min of light exposure.

shown in Fig. 7(a). It can be seen that the slope of the dye degradation graph is upward and steep in the first 45 min of exposure, but it decreases to zero in the second 45 min.

Generally, ozonation in the presence of the TiO$_2$ photocatalyst had the most positive effect on dye degradation. According to Fig. 7 (a), aeration along with ozonation increased the degradation rate so that the highest degradation was seen in the first 20 min. After 20 min of exposure, the most dye degradation belonged to samples (TiO$_2$, MB, Air, O$_3$), (TiO$_2$, MB, O$_3$(Intermittent)), (TiO$_2$, MB, O$_3$(Continuous)), (TiO$_2$, MB, Air) and (TiO$_2$, MB) respectively. Samples (ZnO, MB), (ZnO, MB, O$_3$(Continuous)), and (ZnO, MB, O$_3$(Intermittent)), which were related to ZnO photocatalyst, increased almost linearly with time and had an almost constant slope during 90 min. In addition, the effect of ozonation was minimal in the short term, but it had a positive impact on the amount of degradation after 90 min, Fig. 7(b). In the case of solutions (MB) and (MB, O$_3$), which didn't have photocatalysts, the same relationship was established, and after 90 min, the final degradation of solution (MB, O$_3$), which was ozonated, increased.
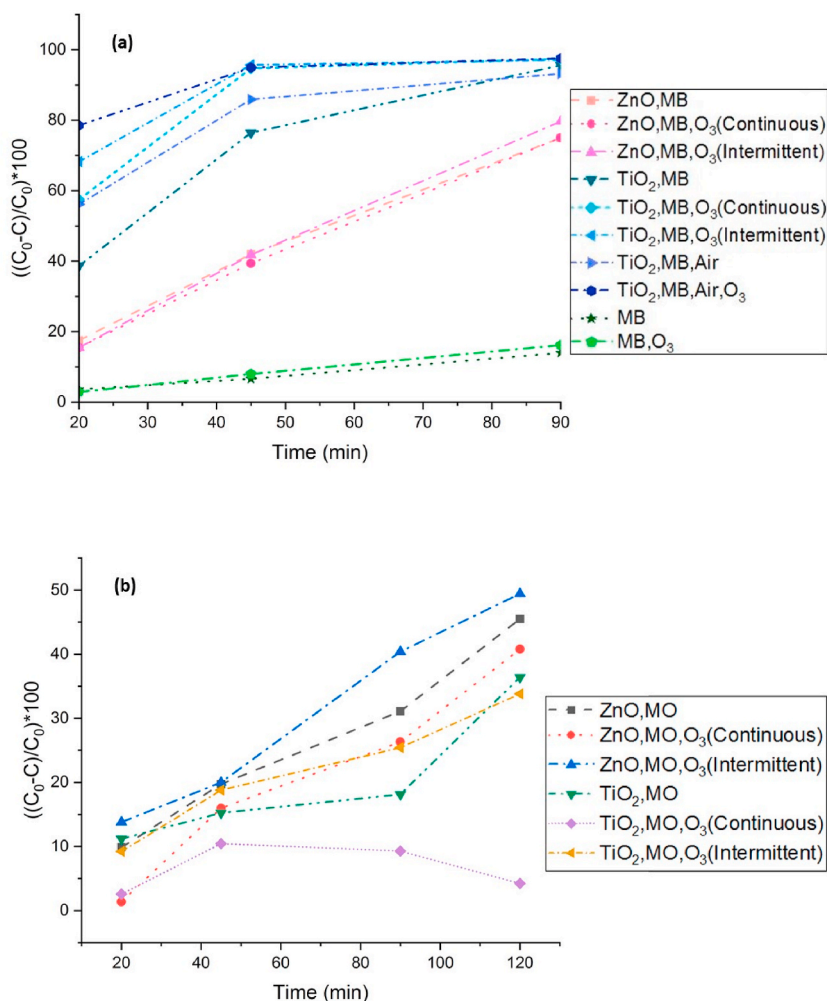
Fig. 7. Graph of percentage of dye degradation by time for (a) MB, and (b) MO.

3.2.2. Effect of air on photocatalytic ozonation

To better analyze the difference in degradation efficiency between intermittent and continuous ozonation, we checked two states for the sample of 10 ppm MB solution in the presence of 0.05 g of TiO_2 in the anatase phase: one where the sample was aerated continuously during light exposure and another where the sample was continuously aerated and ozonated every 5 min with high intensity for 1 min. The results show that the synergy of aeration, ozonation, and photocatalyst created the best dye degradation efficiency, and aeration dramatically increased the speed of dye degradation for ozonated samples. Therefore, it can be concluded that aeration improves the speed of photocatalytic ozonation dye degradation reactions.

3.3. Mechanism discussion of the photocatalytic ozonation process

As mentioned earlier, intermittent ozonation showed better dye degradation efficiency in the first 45 min of exposure, while continuous ozonation showed better degradation after 90 min. The reason is that the reactions related to dye degradation in the presence of ozone require more time. Aeration solved this ozonation problem and achieved 79 % dye degradation after 20 min and 95 % after 45 min.

This result improved the speed and efficiency of photocatalytic dye degradation in the presence of ozone. It showed that providing air and sufficient oxygen in the photocatalytic ozonation process significantly improved dye degradation. Therefore, according to the results obtained in this research, designing a wastewater treatment system that simultaneously uses cold plasma, photocatalyst, ozonation, and aeration technology can significantly improve the speed of wastewater treatment.

Fig. 6(a) shows that the highest amount of dye degradation occurred in the first 20 min of the reaction in the presence of air and photocatalytic ozonation, while after more time, photocatalytic ozonation achieved a significant amount of dye degradation. Aeration significantly increased the speed of the dye degradation reaction, and an increase in dye degradation was seen in the first minutes of the response.

Fig. 8. Sample (TiO$_2$, MB, Air, O$_3$) after 90 min of exposure.

The synergistic effect of air, ozone, and photocatalyst can be seen by comparing the speed of MB degradation reactions, especially in the first 45 min of the response, as shown in Fig. 7.

Fig. 8 shows the dye changes of the tested sample in the presence of photocatalytic ozonation and air, from left to right, at exposure times of 0, 2, 5, 10, 20, 45, and 90 min. A lot of dye was destroyed after 20 min.

4. Conclusion

In this study, the potential of photocatalytic ozonation as an environmentally friendly method for wastewater treatment, capable of efficiently degrading organic pollutants, was investigated. The main findings and contributions of this study can be summarized as follows:

Firstly, the study found that the degradation efficiency of TiO$_2$ and ZnO nanoparticles varied depending on the types of photocatalysts and dyes. Specifically, ZnO nanoparticles were found to be more effective than TiO$_2$ nanoparticles in degrading methyl orange (MO) dye, while TiO$_2$ nanoparticles were more effective in degrading methylene blue (MB) dye.

Secondly, the study found that the photocatalytic activity of both TiO$_2$ and ZnO nanoparticles for the degradation of both MB and MO dyes was enhanced by ozone addition. This was attributed to the generation of more reactive oxygen species and the facilitation of charge transfer.

Thirdly, intermittent ozonation was found to be more effective than continuous ozonation, presumably due to providing more effective contact time and avoiding ozone decomposition. Additionally, the study found that aeration improved the photocatalytic ozonation process by providing more oxygen and enhancing mass transfer and dispersion of ozone in the solution.

However, the study had limitations, including the laboratory scale, volume, and concentration of the dye solutions, and the selection of only two organic dyes (MB and MO) as representative pollutants. Therefore, to validate the photocatalytic ozonation process in natural wastewater treatment plants, further studies are necessary, which test it at a larger scale and with different types of organic pollutants with diverse properties and structures.

CRediT authorship contribution statement

Reyhaneh Nabizadeh: Data curation, Investigation, Writing - original draft. **Rezvaneh Amrollahi:** Data curation, Formal analysis, Methodology, Writing - review & editing. **Bijan Ghafary:** Resources, Validation. **Shahab Norouzian Alam:** Conceptualization, Data curation, Formal analysis, Project administration, Supervision, Validation, Writing - review & editing.

Declaration of competing interest

We declare that we have no known competing financial or personal relationship that could have appeared to influence the work reported in this paper.

References

[1] M. Taie, et al., Comparison of the efficiency of ultraviolet/zinc oxide (UV/ZnO) and ozone/zinc oxide (O3/ZnO) techniques as advanced oxidation processes in the removal of trimethoprim from aqueous solutions, Int. J. Chem. Eng. 2021 (2021) 1–11.

[2] S. Ramasundaram, et al., Synthesis and investigation on synergetic effect of activated carbon loaded silver nanoparticles with enhanced photocatalytic and antibacterial activities, Environ. Res. 233 (2023), 116431.

[3] D. Eissa, et al., Green synthesis of ZnO, MgO and SiO2 nanoparticles and its effect on irrigation water, soil properties, and Origanum majorana productivity, Sci. Rep. 12 (1) (2022) 5780.

[4] Y.H. Kotp, High-flux TFN nanofiltration membranes incorporated with Camphor-Al2O3 nanoparticles for brackish water desalination, Chemosphere 265 (2021), 128999.

[5] Y.H. Kotp, Fabrication of cerium titanate cellulose fiber nanocomposite materials for the removal of methyl orange and methylene blue from polluted water by photocatalytic degradation, Environ. Sci. Pollut. Control Ser. 29 (54) (2022) 81583–81608.

[6] M. Priyadarshini, et al., Advanced oxidation processes: performance, advantages, and scale-up of emerging technologies, J. Environ. Manag. 316 (2022), 115295.

[7] G. Dong, et al., Advanced oxidation processes in microreactors for water and wastewater treatment: development, challenges, and opportunities, Water Res. 211 (2022), 118047.

[8] B. Fatima, et al., Photocatalytic removal of organic dye using green synthesized zinc oxide coupled cadmium tungstate nanocomposite under natural solar light irradiation, Environ. Res. 216 (2023), 114534.

[9] F. Khan, et al., Photocatalytic polymeric composites for wastewater treatment, in: Aquananotechnology, Elsevier, 2021, pp. 467–490.

[10] M. Figueredo, et al., Photocatalytic ozonation in water treatment: is there really a synergy between systems? Water Res. 206 (2021), 117727.

[11] Z. Zafar, R. Fatima, J.-O. Kim, Experimental studies on water matrix and influence of textile effluents on photocatalytic degradation of organic wastewater using Fe–TiO2 nanotubes: towards commercial application, Environ. Res. 197 (2021), 111120.

[12] Y. Liang, et al., Photocatalytic disinfection for point-of-use water treatment using Ti3+ self-doping TiO2 nanoparticle decorated ceramic disk filter, Environ. Res. 212 (2022), 113602.

[13] P. Kasirajan, et al., Fabrication of copper molybdate nanoflower combined polymeric graphitic carbon nitride heterojunction for water depollution: synergistic photocatalytic performance and mechanism insight, Environ. Res. (2023), 116428.

[14] J.M. Coronado, et al., Design of Advanced Photocatalytic Materials for Energy and Environmental Applications, vol. 71, Springer, 2013.

[15] A. Jawed, et al., Photocatalytic metal nanoparticles: a green approach for degradation of dyes, in: Photocatalytic Degradation of Dyes, Elsevier, 2021, pp. 251–275.

[16] D. Koch, S. Manzhos, On the charge state of titanium in titanium dioxide, J. Phys. Chem. Lett. 8 (7) (2017) 1593–1598.

[17] J.E. Haggerty, et al., High-fraction brookite films from amorphous precursors, Sci. Rep. 7 (1) (2017), 15232.

[18] M. Rabbani, et al., Photocatalytic degradation of p-nitrophenol and methylene blue using Zn-TCPP/Ag doped mesoporous TiO2 under UV and visible light irradiation, Desalination Water Treat. 57 (53) (2016) 25848–25856.

[19] A. Janotti, C.G. Van de Walle, Fundamentals of zinc oxide as a semiconductor, Rep. Prog. Phys. 72 (12) (2009), 126501.

[20] S. Mahmud, Synthesis and Characterisation of Zinc Oxide Nanostructures, Doctoral dissertation, Universiti Sains Malaysia, 2008.

[21] M. Naushad, S. Rajendran, E. Lichtfouse, Green Photocatalysts, Springer, 2020.

[22] W.-J. Liu, et al., Composite Fe2O3 and ZrO2/Al2O3 photocatalyst: preparation, characterization, and studies on the photocatalytic activity and chemical stability, Chem. Eng. J. 180 (2012) 9–18.

[23] L. Zhang, et al., Catalytic ozonation mechanisms of Norfloxacin using Cu–CuFe2O4, Environ. Res. 216 (2023), 114521.

[24] N. Moradi, et al., Removal of contaminants of emerging concern from the supernatant of anaerobically digested sludge by O3 and O3/H2O2: ozone requirements, effects of the matrix, and toxicity, Environ. Res. (2023), 116597.

[25] Y. Huang, et al., Iron foam combined ozonation for enhanced treatment of pharmaceutical wastewater, Environ. Res. 183 (2020), 109205.

[26] T. Yang, et al., Enhanced photocatalytic ozonation degradation of organic pollutants by ZnO modified TiO2 nanocomposites, Appl. Catal. B Environ. 221 (2018) 223–234.

[27] I. Fatimah, I. Sumarlan, T. Alawiyah, Fe (III)/TiO2-montmorillonite photocatalyst in photo-Fenton-like degradation of methylene blue, Int. J. Chem. Eng. 2015 (2015).

[28] S.G. Kumar, K.K. Rao, Zinc oxide based photocatalysis: tailoring surface-bulk structure and related interfacial charge carrier dynamics for better environmental applications, RSC Adv. 5 (5) (2015) 3306–3351.

[29] S.-N. Zhu, et al., Catalytic ozonation of basic yellow 87 with a reusable catalyst chip, Chemical engineering journal 242 (2014) 180–186.

[30] K. Mahanpoor, Z. Sharifnezhad, Photo-catalytic ozonation for degrading terephthalic acid in aqueous environment, Archives of Hygiene Sciences 10 (3) (2021) 201–214.

[31] E. Asgari, et al., O3, O3/UV and O3/UV/ZnO for abatement of parabens in aqueous solutions: effect of operational parameters and mineralization/biodegradability improvement, Process Saf. Environ. Protect. 125 (2019) 238–250.

[32] L. Pandian, R. Rajasekaran, P. Govindan, Nanophotocatalytic ozonation of textile dyeing wastewater using Cu-ZnO nanocatalyst and study of reactor influencing parameters, Orient. J. Chem. 35 (1) (2019) 384.

[33] J. Peng, et al., Enhanced photocatalytic ozonation of phenol by Ag/ZnO nanocomposites, Catalysts 9 (12) (2019) 1006.

[34] L. Pandian, R. Rajasekaran, P. Govindan, Synthesis, characterization and application of Cu doped ZnO nanocatalyst for photocatalytic ozonation of textile dye and study of its reusability, Mater. Res. Express 5 (11) (2018), 115505.

[35] A. Ikhlaqa, et al., Combined UV catalytic ozonation process on iron loaded peanut shell ash for the removal of methylene blue from aqueous solution, Desalination Water Treat. 200 (2020) 231–240.

[36] C. Wei, et al., Ozonation in water treatment: the generation, basic properties of ozone and its practical application, Rev. Chem. Eng. 33 (1) (2017) 49–89.

[37] A.A.S. Alahl, et al., Synthesis of a novel photocatalyst based on silicotitanate nanoparticles for the removal of some organic matter from polluted water, Catalysts 13 (6) (2023) 981.

[38] M. Khalil, M.A. Sayed, Y.H. Kotp, Gamma radiation-induced synthesis of TiO2 immobilized on polyacrylonitrile nanocomposite for gallium, strontium and rubidium ions separation from aqueous solutions, Radiat. Phys. Chem. (2023), 111085.

[39] R.A. Lance, Optical Analysis of Titania: Band Gaps of Brookite, Rutile and Anatase, 2018.

[40] X. Yuan, et al., Preparation and application of immobilized surfactant-modified PANi-CNT/TiO2 under visible-light irradiation, Materials 10 (8) (2017) 877.

[41] I. Khan, et al., Review on methylene blue: its properties, uses, toxicity and photodegradation, Water 14 (2) (2022) 242.

[42] L. Wu, et al., Study on the adsorption properties of methyl orange by natural one-dimensional nano-mineral materials with different structures, Sci. Rep. 11 (1) (2021), 10640.

[43] R. Bhattacharjee, et al., Effective materials in the photocatalytic treatment of dyestuffs and stained wastewater, in: Trends and Contemporary Technologies for Photocatalytic Degradation of Dyes, Springer, 2022, pp. 173–200.

[44] V.-P. Dinh, et al., Insight into the adsorption mechanisms of methylene blue and chromium (III) from aqueous solution onto pomelo fruit peel, RSC Adv. 9 (44) (2019) 25847–25860.

[45] S. Zargari, et al., Enhanced visible light photocurrent response and photodegradation efficiency over TiO2–graphene nanocomposite pillared with tin porphyrin, J. Colloid Interface Sci. 466 (2016) 310–321.

[46] R. Rahimi, M. Rabbani, S.S. Moghaddam, Application of N, S-codoped TiO2 photo-catalyst for degradation of methylene blue, in: Proceedings of the 16th International Conference on Synthetic Organic Chemistry, ECSOC-16'12), 2012.

[47] L.-Z. Deng, et al., Emerging chemical and physical disinfection technologies of fruits and vegetables: a comprehensive review, Crit. Rev. Food Sci. Nutr. 60 (15) (2020) 2481–2508.

[48] S.N. Manjunath, et al., Recent case studies on the use of ozone to combat coronavirus: problems and perspectives, Environ. Technol. Innov. 21 (2021) 101313.

[49] H. Jakob, M.K. Kim, Generation of non-thermal plasmas over large and complex surfaces, Plasma Research Express 2 (3) (2020), 035010.

[50] M. Qasim, M.S. Rafique, R. Naz, Water purification by ozone generator employing non-thermal plasma, Mater. Chem. Phys. 291 (2022), 126442.

[51] M. Tański, et al., Ozone generation by surface dielectric barrier discharge, Appl. Sci. 13 (12) (2023) 7001.

[52] J.-h. Park, et al., Space sterilization effect through high-density plasma ozone using DBD device, Journal of Electrical Engineering & Technology 17 (5) (2022) 2771–2778.

[53] T. Theivasanthi, M. Alagar, Titanium Dioxide (TiO2) Nanoparticles XRD Analyses: an Insight, 2013 arXiv preprint arXiv:1307.1091.

[54] S. Talam, S.R. Karumuri, N. Gunnam, Synthesis, Characterization, and Spectroscopic Properties of ZnO Nanoparticles, vol. 2012, International Scholarly Research Notices, 2012.

[55] A. Šuligoj, et al., Synergism in TiO2 photocatalytic ozonation for the removal of dichloroacetic acid and thiacloprid, Environ. Res. 197 (2021), 110982.